Catalysis Science & Technology

Accepted Manuscript

This article can be cited before page numbers have been issued, to do this please use: R. Assis dos Santos, A. Ben Hassine, P. J. Sanches Filho, M. J. Neiva Correia and P. S. F. Mendes, *Catal. Sci. Technol.*, 2026, DOI: 10.1039/D6CY00118A.

ROYAL SOCIETY OF CHEMISTRY

rsc.li/catalysis

View Article Online
DOI: 10.1039/D6CY00118A

COMMUNICATION

Continuous-flow hydroprocessing of long-chain fatty acids: reaction pathways and the impact of lignin-derived aromatics towards efficient deoxygenation

Received 00th January 20xx,
Accepted 00th January 20xx

DOI: 10.1039/x0xx00000x

Rita Assis dos Santos,*[ab] Arij Ben Hassine,[b] Pedro José Sanches Filho,[b] M. Joana Neiva Correia,[ac] and Pedro S. F. Mendes*[ab]

This study establishes oleic acid reaction pathways under long-term continuous-flow hydroprocessing, highlighting the metal and acid sites roles for efficient deoxygenation. At industrially relevant conversions, guaiacol co-feeding, despite accelerating catalyst deactivation, largely preserved the oleic acid-derived fingerprint (83 wt. % of the organic fraction) with mixed-origin products accounting for the remainder. These findings allow tailoring sustainable aviation fuel composition while diversifying non-conventional feedstocks.

Introduction

The carbon neutrality of the aviation sector remains an open challenge in the climate transition. Aircraft require high-energy-density and intrinsically safe fuels, properties which liquid hydrocarbons deliver today, while batteries or gas fuels (e.g., hydrogen) will not apparently achieve those in the near future [1–3]. Sustainable Aviation Fuels (SAFs), derived from renewable or waste-based sources, are therefore a key route to reducing the global warming footprint of aircraft [1,3–6]. SAFs have a similar chemical composition to conventional jet fuel (including iso-paraffins, paraffins, aromatics and cycloalkanes), making them compatible with existing infrastructure [3,4]. Despite strong policy support (e.g., *ReFuelEU*, which targets 6 % and 20 % of SAF incorporation by 2030 and 2035, respectively [1]), global SAF production remains limited and below expectations [1,2,4].

Among the approved production routes, Hydroprocessed Esters and Fatty Acids (HEFA) is currently the most technologically mature and commercially deployed process [1–4,6]. HEFA converts mainly lipidic feedstocks, such as vegetable oils, animal fats, or used cooking oils, into hydrocarbons (HC) through deoxygenation (primarily acid-catalysed [7] hydrodeoxygenation (HDO), metal-catalysed [7,8] decarboxylation (DCO_x) and decarbonylation (DCO)), followed by acid-catalysed [7,9] hydrocracking (HCK) and hydroisomerisation (HDI) reactions [4–6,10]§.

The scalability of HEFA fuels is nevertheless constrained by the limited global availability and cost of lipidic feedstocks [1,2,5,6], motivating research towards incorporating more abundant resources, such as lignocellulosic biomass [2,3,6,10].

The simultaneous hydroprocessing of lipidic and lignocellulosic-derived feedstocks, potentially in existing refinery units, is thus a promising strategy [10]. This integrated approach not only diversifies feedstock supply chains and potentially reduces costs, but also enables tuning of paraffinic and aromatics fractions to meet jet fuel specifications, including cold flow and aromatic content requirements [1,10].

Nonetheless, lipidic and lignocellulosic-derived feedstocks differ significantly in chemical structure, with long-chain fatty acids and oxygenated aromatic compounds, respectively. These differences may result in unexpected interactions when processed together. In other words, mixture effects, impacting, e.g., deoxygenation efficiency or product selectivity, may arise under simultaneous hydroprocessing [11].

While the individual hydroprocessing of representative model compounds, such as oleic acid and guaiacol, has been studied often in batch systems [7,12–17], rather than in continuous-flow [18–21], mixture effects are yet to be established. Batch conversion blends of bio-oil and waste/vegetable oils over acidic (Ni)CoMo catalysts (mainly investigating fuel yields, coke formation and solvent effects), has shown that lignin-derived compounds influence coke formation and overall product distribution [22,23]. Under

[a] Departamento de Engenharia Química, Instituto Superior Técnico, Universidade de Lisboa, Av. Rovisco Pais, 1049-001 Lisboa, Portugal.
Email: rita.assis.santos@tecnico.ulisboa.pt (Rita Assis dos Santos), pedro.f.mendes@tecnico.ulisboa.pt (Pedro S. F. Mendes)
[b] Centro de Química Estrutural, Institute of Molecular Sciences, Instituto Superior Técnico, Universidade de Lisboa, Av. Rovisco Pais, 1049-001 Lisboa, Portugal.
[c] Centro de Recursos Naturais e Ambiente, Instituto Superior Técnico, Universidade de Lisboa, Av. Rovisco Pais, 1049-001 Lisboa, Portugal.

Electronic Supplementary Information available: experimental section, review and analysis of oleic acid reaction pathways, Fig. S1 – S15, Table S1 – S4, Eq. S1 – S3 and additional references. See DOI: 10.1039/x0xx00000x

View Article Online
DOI: 10.1039/D5CY00148A

continuous operation over non-acidic (Ni)CoMo catalysts, mixtures of mono-substituted oxygenated aromatics with short-chain carboxylic acids and aldehydes exhibited shifts in conversion (with different magnitudes) to higher temperatures due to competitive adsorption, with carboxylic acids exerting the strongest impact on the conversion of other compounds [19]. Similarly, studies on lauric acid/anisole and indole-containing mixtures over acidic and non-acidic nickel-based catalysts (e.g., NiMo) demonstrated the suppression of C-O cleavage of anisole until the consumption of other reactants. This led to reduced deoxygenated HC yields in the presence of carboxylic acids or nitrogen-containing compounds [11,24]. Furthermore, in lauric acid/indole mixtures, there was an increase in the production of condensation products [11]. Additionally, multiscale and microkinetic modelling approaches have been applied to analyse reaction mechanisms and transport phenomena in hydroprocessing systems for different compound families [25,26]. Collectively, these studies demonstrate that co-feeding chemically distinct compounds can modify conversion behaviour and induce competition or inhibitory effects between feedstocks. However, products are often analysed as bulk HC lumps, hindering a comprehensive analysis of the underlying reaction pathways. Consequently, an understanding of how mixture effects influence deoxygenation routes under continuous operation remains limited.

The objective of this work is therefore to evaluate potential mixture effects arising from the simultaneous hydroprocessing of chemically distinct model compounds, supported by an experimental understanding of individual reaction pathways under industrially relevant (i.e., continuous, high conversion) operation. First, the conversion-controlled reaction pathways for oleic acid are established over a long-term experiment (Time On Stream (TOS) > 72 h, as defined in Electronic Supplementary Information (ESI) Section 1.3) under fixed operating conditions (T = 360 ºC, P = 40 bar, H_2/oleic acid = 1000 NmL/mL, Weight Hourly Space Velocity (WHSV) = 9.4 h^{-1}) and catalyst formulation (reference bifunctional 20Ni/HZSM-5 catalyst). This then serves as a basis for investigating mixture effects in simultaneous hydroprocessing with guaiacol, via the impact of the oxygenated aromatic on fatty acid conversion and organic product distribution under continuous operation.

Oleic acid single-feed

To establish a comprehensive pathway scheme of the cascade reactions, (i) conversion was followed over an extended TOS to capture key intermediates and products, and (ii) a bifunctional catalyst was selected to explore the metal and acid functions. Moreover, to ensure intrinsically reproducible results, the catalyst was prepared by a simple mechanical mixture of two commercially available materials (vide ESI Section 1.2). Details on feedstocks, catalyst preparation and characterisation, experimental setup, product analysis and data treatment are provided in ESI Section 1.

Reaction pathways

The reaction pathways were determined by combining product distributions (over different conversions) with stoichiometric analysis based on molar flowrates (vide ESI, Section 2.2) and ultimately validated against individual pathways reported in literature (vide ESI, Section 2.1). Therefore, all the reaction pathways were determined based on experimental data. The active sites primarily catalysing each reaction were exclusively literature-based and will not be presented here (vide ESI, Table S3). Although not the focus of this study, primary reaction mechanisms, when available, are also disclosed in ESI Section 2.1, based on literature.

The proposed reaction network for oleic acid hydroprocessing over a bifunctional catalyst is presented in Fig. 1. It is described following the progression of the cascade reactions through key oxygenated intermediates and ultimately culminating in deoxygenated HC. Note that according to the evidence collected over various experiments (vide ESI, Fig. S11), catalyst deactivation over time does not majorly affect the reaction pathways discussed hereafter, as it mainly leads to the suppression of hydrogenolysis and HCK (further discussion in ESI Section 2.3).

Initial hydrogenation of unsaturated fatty acids was identified as a major (vide ESI, Fig. S8) and relatively fast step [7,27,28]. This is consistent with energetic considerations, since the activation barrier for C=C hydrogenation (614 kJ/mol) is lower than the C=O bond cleavage (799 kJ/mol) [14]. Linoleic acid was first hydrogenated to oleic acid and subsequently to stearic acid (Reactions 1 – 2 in Fig. 1), considering its relative abundance decreased from 22 wt. %[§§] to 0.3 % wt. % upon conversion increase (vide ESI, Fig. S8). The formation of stearic acid (< 25 wt. %) establishes a central saturated fatty acid from which subsequent oxygenated species can be generated. At lower conversions (< 90 wt. %), these include octadecanol, stearyl stearate and dioctadecyl ether (vide ESI, Fig. S7), which can possibly be further converted.

Low ester amounts (< 8 wt. %) were detected experimentally (vide ESI, Fig. S8). Thus, esterification between stearic acid and octadecanol (Reaction 3 in Fig. 1) [25,27,29] represents a minor route, bridging key fatty-acid and alcohol intermediates within the reaction network. Nevertheless, esters are reported in the literature to be reactive under hydroprocessing conditions and may undergo further transformations, such as dehydration to octadecene [8,27]. Etherification proceeded via dehydration of octadecanol molecules (Reaction 4 in Fig. 1, right-hand side), forming low dioctadecyl ether amounts (< 1 wt. %) and water [25,30]. Their relative abundance decreased with increasing conversion (vide ESI, Fig. S8), indicating that ether formation is a minor route rather than a key intermediate step. Compared to esters, ethers are less reactive, being thus less likely to undergo further reactions.

Octadecanal and octadecanol (< 1 wt. %) can be produced from stearic acid hydrogenation (Reactions 5 – 6 in Fig. 1) and subsequently interconvert through hydrogenation/dehydrogenation (Reaction 7 in Fig. 1)

View Article Online
DOI: 10.1039/D6CY00118A

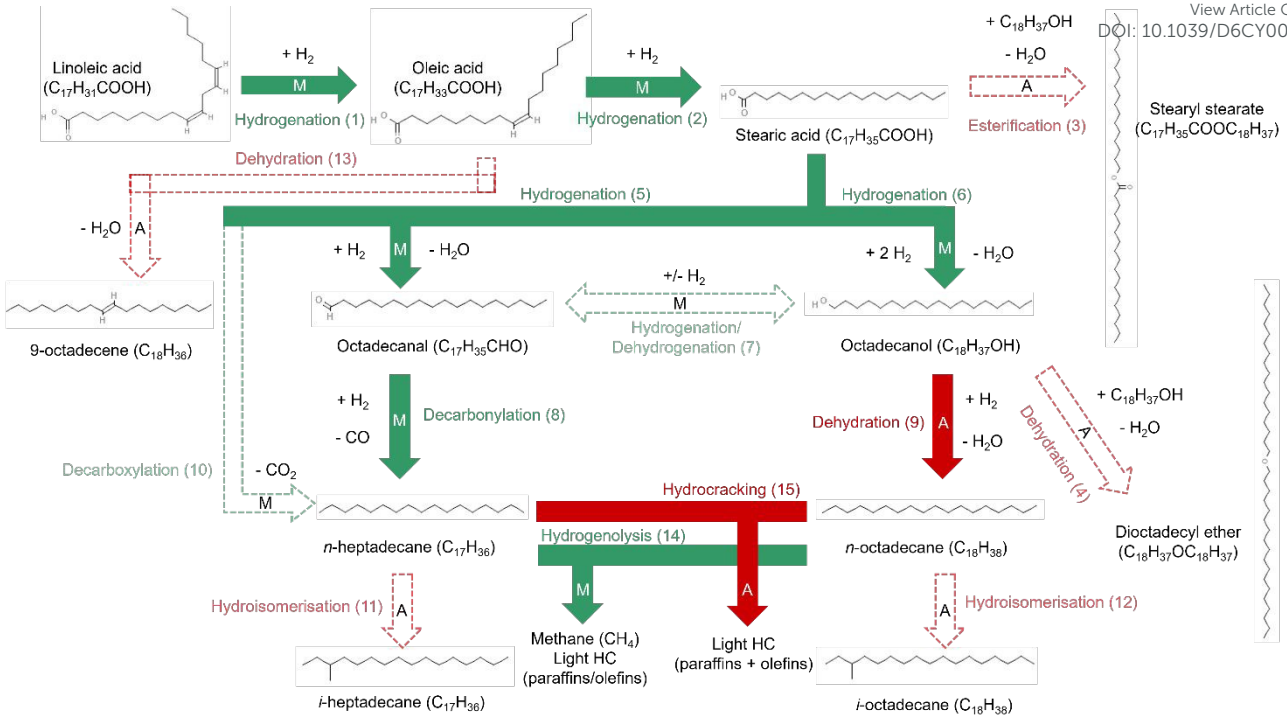

Fig. 1 Proposed reaction pathways for oleic acid hydroprocessing over 20Ni/HZSM-5. Green arrows represent reactions primarily catalysed by metal sites (M), while red arrows represent reactions primarily catalysed by acid sites (A). Solid arrows correspond to major pathways, whereas dashed, lighter coloured arrows correspond to minor pathways. Reaction pathways are experimentally determined, and active sites are exclusively literature-based (vide ESI, Table S3).

[7,8,25,29], forming a central reaction node from which two major deoxygenation routes subsequently emerge. Octadecanal can undergo DCO to yield the corresponding C_{17} HC (> 30 wt. %) (Reaction 8 in Fig. 1) [7,27,28], while octadecanol can be dehydrated to produce the corresponding C_{18} HC (> 10 wt. %) (Reaction 9 in Fig. 1) [7,28]. In addition to these pathways, stearic acid can be directly converted to heptadecane via DCO_x (Reaction 10 in Fig. 1) [7]. This route was identified as minor based on gaseous product analysis, where CO_2 amounts never exceeded 5 wt. % of the gaseous products (vide ESI, Fig. S10), and is consistent with previous studies [31]. Both C_{17} and C_{18} HC can subsequently undergo HDI (Reactions 11 – 12 in Fig. 1) [7,27], though this reaction remained limited, given the low isomer to HC ratios (ca. 0.1, vide ESI, Fig. S12).

Interestingly, our results suggest possible direct dehydration of oleic acid to octadecene (Reaction 13 in Fig. 1) [27] without prior hydrogenation (vide ESI, Section 2.3). Hydrogenolysis and HCK (Reactions 14 – 15 in Fig. 1) represent additional important pathways [7,12,13,27,28]. In hydrogenolysis, either paraffins or olefins can be produced depending on H_2 availability, though under hydroprocessing conditions, olefins tend to hydrogenate back to paraffins [32]. Cracking products may also include paraffin-paraffin or paraffin-olefin pairs. These smaller fragments may further recombine [7], accounting for the formation of HC with carbon chains larger than C_{18} HC, at most 13 wt. % (not depicted in Fig. 1, vide ESI, Fig. S9).

Role of active sites on the reaction pathways

The network proposed here integrates these individual reactions into a unified cascade, capturing both major and minor pathways, over a representative bifunctional catalyst. As many of these reactions have been studied in detail separately (vide ESI, Table S3 and Section 2.1), this active site-specific knowledge was leveraged to specify the roles of metal and acid sites in the overall deoxygenation network (see arrows' inner text in Fig. 1).

Under the studied conditions, the results point towards a reaction network governed by metal-catalysed pathways. The HC fraction consistently exhibited a predominance of C_{17} HC (> 30 wt. %) (vide ESI, Fig. S9), and CO/CO_2 were detected in the gas phase (vide ESI, Fig. S10), indicating that metal-catalysed DCO/DCO_x prevailed over acid-catalysed HDO. This behaviour aligns with a previous single-feed batch study using analogous catalysts and feedstocks, where metal site-dominated systems favoured alkane formation [27]. Furthermore, other studies also reported that nickel-based catalysts and high temperatures (particularly 375 ºC [14]) promote DCO/DCO_x over HDO [12,28]. The selectivity towards metal-catalysed reactions, despite the presence of strong Brønsted acidity in ZSM-5, can be tentatively attributed to the high metal loading and limited accessibility of Brønsted acid sites, considering the larger kinetic diameter of oleic acid (8 Å [33]) relative to the ZSM-5 pore diameter (5.1 – 5.6 Å [34]).

Guaiacol co-feeding

To isolate the specific impact of guaiacol co-feeding without introducing additional variables, the same catalyst formulation and operating conditions as in the conversion-controlled oleic acid single-feed experiment were maintained (described

above). Particularly, the oleic acid partial pressure at the reactor inlet was preserved by replacing part of the excess H_2 with guaiacol, thereby avoiding spurious effects in the reaction rates. An 87/13 oleic acid/guaiacol mass ratio was selected to reflect industrially relevant SAF blending targets (6 % and 20 % by 2030 and 2035, respectively, according to *ReFuelEU* [1]) while ensuring sufficient product concentration for reliable quantification.

Feedstock conversion

Feedstock conversion profiles§§§ are presented in Fig. 2. In the presence of guaiacol, fatty acid conversion was consistently lower than in the single-feed experiment. This effect was accompanied by a more pronounced relative abundance of stearic acid (vide ESI, Fig. S14a), indicating a lower overall reaction progression under simultaneous hydroprocessing. Guaiacol itself exhibited lower conversions compared to the fatty acids, below 70 % over the 72 h period. Notably, both fatty acids and guaiacol conversions declined by approximately 40 % (from 91 % to 51 % and from 67 % to 39 %, respectively) during simultaneous hydroprocessing, which is roughly twice the decline observed for fatty acids under single-feed conditions (from 99 % to 83 %).

Concerning the initial fatty acid conversion (i.e., at TOS approaching zero), the evidence is limited to the first sampling point and includes a certain time lag. Still, it seems that in simultaneous hydroprocessing, fatty acid conversion is lower than in the single-feed. This suggests the possibility of competitive adsorption between oleic acid and guaiacol for active sites. Both oleic acid and guaiacol hydroprocessing pathways require metal and acid sites for efficient deoxygenation (vide *Reaction pathways* section). Although several of guaiacol's reactions are acid-catalysed, they also involve the metal function to promote deoxygenation [16,35,36]. This means that guaiacol's strong adsorption on the catalyst surface [21] could hinder fatty acid conversion. Although over simpler model compounds (anisole and heptanoic acid), a previous study has also shown that co-feeding carboxylic acids and aromatic compounds shifts

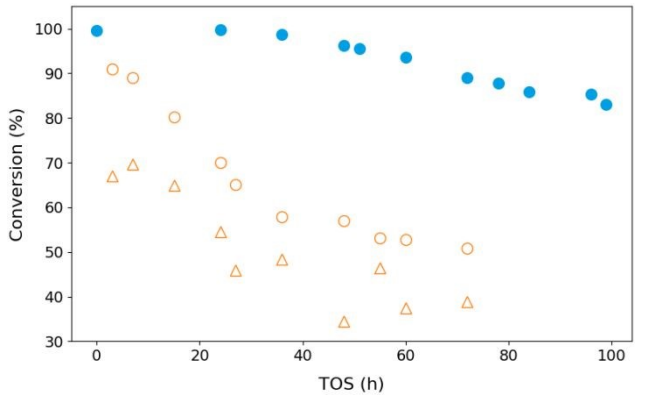

Fig. 2 Fatty acid and guaiacol conversion for single-feed (oleic acid) and simultaneous hydroprocessing (oleic acid/guaiacol mixture, 87/13 mass ratio) experiments over 20Ni/HZSM-5 (P = 40 bar, T = 360 ºC, H_2/oleic acid = 1000 NmL/mL, WHSV = 9.4 h^{-1}). Single-feed experiment: fatty acid conversion (●); simultaneous hydroprocessing: fatty acid conversion (○), guaiacol conversion (△). Fatty acid conversion includes contributions from linoleic acid, oleic acid and stearic acid.

conversion due to competitive adsorption on active sites [19].

Concerning deactivation, Fig. 2 also shows two distinct deactivation profiles between the single-feed and simultaneous hydroprocessing. In the single-feed experiment, an S-shaped curve, with an initial induction period with limited impact, followed by a sharp increase in the slope of conversion variation over time, was observed, indicating a cumulative or sequential effect [37]. In contrast, during simultaneous hydroprocessing, the conversion immediately dropped from low TOS, with the slope progressively decreasing over time, in an exponential decay-like fashion. This accelerated and more severe deactivation observed in the presence of guaiacol points towards its potential role as a deactivation precursor. Polymerisation of unsaturated phenolic compounds, such as guaiacol, is considered one of the main causes for coke formation in hydroprocessing, through the production of condensed polyaromatic species [22,23,35,38]. Other continuous-flow studies using oxygenated aromatics and nickel-based catalysts also reported fast catalyst deactivation (within the first 5 h) [39]. On the other hand, fatty acids alone are not considered primary coke precursors and typically require the prior formation of by-products [38].

In summary, based on the feedstock conversion profiles, guaiacol co-feeding led to overall lower fatty acid conversion along with a faster and more severe catalyst deactivation, compared with the single-feed oleic acid experiment.

Organic product distribution

To further elucidate mixture effects in terms of preferred reaction pathways, the organic product distribution of oleic acid was evaluated at iso-conversion under high (ca. 90 %) and moderate (ca. 50 %) conversion levels, as depicted in Fig. 3 (a and b), respectively. Different conversion levels were achieved by following the evolution with TOS under otherwise identical conditions or by varying WHSV. To prevent any interference of guaiacol-derived products, the distribution focuses on C_8+ HC products. This also limits the influence of catalyst deactivation on the observed products (and pathways) as the key differences are chiefly C_7- HC (formed via hydrogenolysis and HCK, vide ESI, Section 2.3). High conversion conditions are discussed first, as they allow for a direct comparison of oleic acid-derived products without interference from mixed-origin condensation products, which are only observable at lower conversions.

Regarding the high conversion case in Fig. 3a, the overall product distributions observed under single-feed and simultaneous hydroprocessing conditions were remarkably similar (the minor variations were deemed rather negligible when accounting for experimental uncertainty). This demonstrates the robustness of oleic acid reaction pathways even in the presence of oxygenated aromatics. For the moderate conversion scenario in Fig. 3b, a similar overall fingerprint was observed, with apparent differences in the carboxylic acid fraction (represented by the striped bars). Under these conditions, mixed-origin products (namely phenolic esters and aliphatic ketones) were detected (vide ESI, Section 3), whereas they were absent at high conversion, making up for

View Article Online
DOI: 10.1039/D6CY00118K

the largest share of product distribution gaps, namely in the acids and C_{17} HC fractions (represented by the dotted bars).

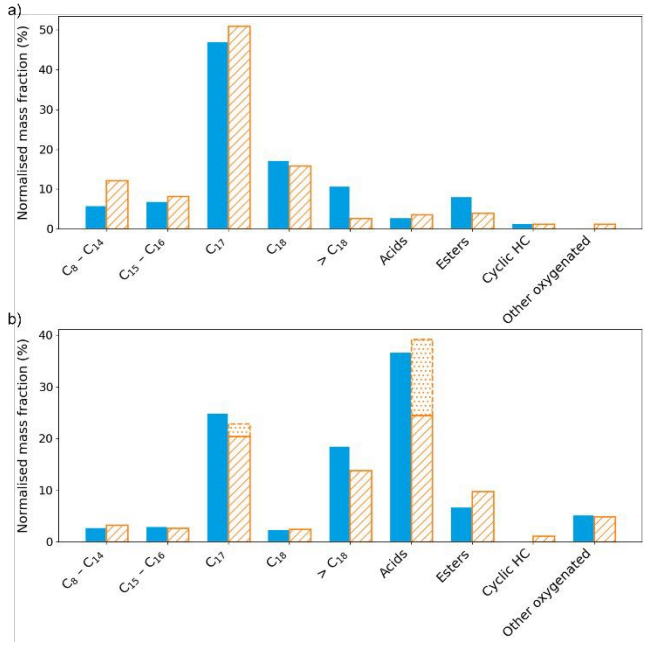

Fig. 3 Product distribution evolution in the organic phase for single-feed (oleic acid) and simultaneous hydroprocessing (oleic acid/guaiacol mixture, 87/13 mass ratio) experiments over 20Ni/HZSM-5 (excluding linoleic, oleic and stearic acids): a) high conversion (ca.90 %); b) moderate conversion (ca. 50 %). Single-feed: oleic acid-derived products ( ); simultaneous hydroprocessing: oleic acid-derived products ( ); estimated mixed-origin products, namely phenolic esters and aliphatic ketones ( ). Common operating conditions: P = 40 bar, T = 360 ºC, H_2/oleic acid = 1000 NmL/mL. High conversion conditions: WHSV = 9.4 h^{-1}; single-feed at TOS = 60 h; simultaneous hydroprocessing at TOS = 3 h. Low conversion conditions: single-feed at WHSV = 19.0 h^{-1} and TOS = ~ 14 h; simultaneous hydroprocessing at WHSV = 9.4 h^{-1} and TOS = 72 h.

Overall, these results indicate that although catalyst deactivation strongly influences conversion levels, it does not significantly affect the lipid-derived product distribution (over the studied operating conditions). This is consistent with single-feed observations (vide ESI, Fig. S11) that deactivation primarily suppressed hydrogenolysis and HCK reactions, a classical effect in HC hydroprocessing [9,32]. Since the light HC fractions associated with these pathways are comparable in both experiments in Fig. 3 (a and b), the differences observed are governed by conversion levels rather than by catalyst deactivation.

Therefore, over this representative bifunctional catalyst and conversion levels, the primary mixture effect at the product level when co-feeding guaiacol is the formation of intermediate mixed-origin products, rather than a fundamental change in oleic acid reaction pathways.

Oleic acid co-feed reaction pathways

Taking the previous section's results into account, the proposed network can be further validated at moderate conversions. At such conversions, the product distribution was dominated by oxygenated intermediates, particularly stearic acid, which is a key intermediate in oleic acid hydroprocessing. As conversion increased, the cascade reactions (presented in Fig. 1) leading to deoxygenated HC were favoured, resulting in higher HC yields and lower acid ones. This trend illustrates how the extension of the reaction network drives the system from oxygenated species towards fully deoxygenated products.

Despite these conversion-dependent changes, the HC fraction consistently exhibited a predominance of C_{17} HC (vide ESI, Fig. S14a), indicating that metal-catalysed DCO/DCO_x were the major hydroprocessing pathways, rather than acid-catalysed HDO, as in the single-feed experiment (vide *Role of active sites on reaction pathways* section). Fig. 3 also depicts the formation of mixed-origin products at lower conversions, providing additional insights into chemical reactivity between oleic acid and guaiacol. To the best of our knowledge, the formation of these mixed-origin species has not been previously reported. To further explore these results, tentative reaction pathways were proposed (vide ESI, Fig. S15), inferred from the relative abundance of reactants, as well as the molecular structure of potential reactants and their textbook functional group reactivity. Phenolic esters, the main mixed-origin products (15 wt. %), are likely formed via esterification reactions, which require a carboxylic group and an alcohol function [40]. Guaiacol's hydroxyl group provides the alcohol function, while oleic acid supplies the carboxylic acid functional group. Aliphatic ketones (2 wt. %) may result from coupling reactions between ketones and olefins [41]. Cyclohexanone (formed during guaiacol hydroprocessing) reacts with unsaturated HC such as heptadecene (generated from oleic acid hydroprocessing), which offers reactive sites for C-C bond formation with the cyclohexanone structure.

Conclusions

Under the studied operating conditions in long-term hydroprocessing over a representative bifunctional catalyst (20Ni/HZSM-5), the cascade reactions were initiated by rapid hydrogenation to stearic acid, considering its relative abundance decreased as fatty acid conversion increased. This was followed by metal-catalysed decarbonylation to C_{17} HC, the predominant product (> 30 wt. % of the organic fraction) and acid-catalysed dehydration to C_{18} HC (> 10 wt. % of the organic fraction). During simultaneous hydroprocessing with guaiacol, despite accelerated catalyst deactivation, evidenced by a distinct conversion profile, the oleic acid-derived fingerprint (83 wt. %) was largely preserved over a wide conversion range (ca. 50 – 90 %), demonstrating the robustness of oleic acid reaction pathways even in the presence of oxygenated aromatics. Mixture effects were primarily reflected in the moderate formation of mixed-origin products (17 wt. % of the organic fraction), such as phenolic esters and aliphatic ketones at lower conversion levels (ca. 50 %), rather than changes in HC selectivity. In summary, oleic acid hydroprocessing resulted in efficient deoxygenation through a predominantly metal site-dominated reaction network. While the experimental data is limited to the catalyst selected and operating conditions covered, these allowed to assess simultaneously both metal and acid sites over a rather wide conversion range (ca. 50 – 99 %), increasing the generalisation potential of the reaction network

to other continuous systems. These findings highlight the potential of simultaneous processing strategies to diversify feedstocks while controlling sustainable aviation fuel composition.

Author contributions

Rita Assis dos Santos: Conceptualization, Data curation, Investigation, Methodology, Visualization, Writing – original draft. Arij Ben Hassine: Writing – review & editing. Pedro José Sanches Filho: Data curation, Investigation, Methodology. M. Joana Neiva Correia: Methodology, Supervision, Writing – review & editing. Pedro S. F. Mendes: Conceptualization, Methodology, Supervision, Writing – review & editing.

Conflicts of interest

There are no conflicts to declare.

Data availability

The raw and processed data for Fig. 2 – 3 are openly available in a FAIR format in *Zenodo* at https://doi.org/10.5281/zenodo.18313041. Details of data postprocessing are provided in Section 1 of ESI. Additional processed data supporting this study are included in ESI.

Acknowledgements

The authors acknowledge funding from Fundação para a Ciência e Tecnologia (FCT) through CQE (UID/00100/2025; UID/PRR/00100/2025), IMS (LA/P/0056/2020) and CERENA (UID/04028/2025). Funding was also provided by the European Union (*NextGenerationEU*) through the Portuguese Government via the Agenda Moving2Neutrality no. C644927397-00000038, project no. 32. The authors also thank all the M2N project team for their insightful feedback.

Notes and references

§Across literature, this conversion process is often described using different but overlapping terms, including hydroprocessing, hydroconversion, hydrotreatment or hydrodeoxygenation. To facilitate cross-disciplinary communication, in this work, hydroprocessing is employed and encompasses all hydrogen-assisted catalytic upgrading reactions in SAF production.

§§All the mass fractions subsequently presented are referred to the liquid organic phase in the C_{7+} fraction (vide ESI, Section 1.4), except when explicitly stated otherwise.

§§§Owing to the fast interconversion between fatty acids (i.e., linoleic, oleic and stearic acids, see the previous section), a fatty acid conversion was employed as a measurement of overall reaction extent for oleic acid deoxygenation.

[1] Qasem NAA, Mourad A, Abderrahmane A, et al. A recent review of aviation fuels and sustainable aviation fuels. J Therm Anal Calorim 2024;149:4287–312. https://doi.org/10.1007/s10973-024-13027-5.

[2] Watson MJ, Machado PG, da Silva AV, et al. Sustainable aviation fuel technologies, costs, emissions, policies, and markets: A critical review. J Clean Prod 2024;449:141472. https://doi.org/10.1016/j.jclepro.2024.141472.

[3] Raji AM, Manescau B, Chetehouna K, et al. Overview of combustion and emission characteristics of sustainable aviation fuels and standard JET A-1 fuel. Fuel 2025;402:136011. https://doi.org/10.1016/j.fuel.2025.136011.

[4] Wang B, Ting ZJ, Zhao M. Sustainable aviation fuels: Key opportunities and challenges in lowering carbon emissions for aviation industry. Carbon Capture Science & Technology 2024;13:100263. https://doi.org/10.1016/j.ccst.2024.100263.

[5] Arias A, Nika C-E, Vasilaki V, et al. Assessing the future prospects of emerging technologies for shipping and aviation biofuels: A critical review. Renewable and Sustainable Energy Reviews 2024;197:114427. https://doi.org/10.1016/j.rser.2024.114427.

[6] Borrill E, Koh SCL, Yuan R. Review of technological developments and LCA applications on biobased SAF conversion processes. Frontiers in Fuels 2024;2. https://doi.org/10.3389/ffuel.2024.1397962.

[7] Žula M, Grilc M, Likozar B. Hydrocracking, hydrogenation and hydro-deoxygenation of fatty acids, esters and glycerides: Mechanisms, kinetics and transport phenomena. Chemical Engineering Journal 2022;444:136564. https://doi.org/10.1016/j.cej.2022.136564.

[8] Kiméné A, Wojcieszak R, Paul S, et al. Catalytic decarboxylation of fatty acids to hydrocarbons over non-noble metal catalysts: the state of the art. Journal of Chemical Technology & Biotechnology 2019;94:658–69. https://doi.org/10.1002/jctb.5776.

[9] Weitkamp J. Catalytic Hydrocracking—Mechanisms and Versatility of the Process. ChemCatChem 2012;4:292–306. https://doi.org/10.1002/cctc.201100315.

[10] Calderon Rosales O, Tao L, Abdullah Z, et al. Sustainable Aviation Fuel (SAF) State-of-Industry Report: State of SAF Production Process. 2024.

[11] Kikhtyanin O, Kubička D. Understanding peculiarities in the simultaneous HDO and HDN during the hydroconversion of indole in its mixture with lauric acid and anisole over a NiMo/Al2O3catalyst – An important step towards efficient

bio-oil upgrading. Fuel 2026;406:137144. https://doi.org/10.1016/j.fuel.2025.137144.

[12] Song M, Zhang X, Chen Y, et al. Hydroprocessing of lipids: An effective production process for sustainable aviation fuel. Energy 2023;283. https://doi.org/10.1016/j.energy.2023.129107.

[13] Mäki-Arvela P, Martínez-Klimov M, Murzin DYu. Hydroconversion of fatty acids and vegetable oils for production of jet fuels. Fuel 2021;306:121673. https://doi.org/10.1016/j.fuel.2021.121673.

[14] Rahmawati Z, Santoso L, McCue A, et al. Selectivity of reaction pathways for green diesel production towards biojet fuel applications. RSC Adv 2023;13:13698–714. https://doi.org/10.1039/d3ra02281a.

[15] Jin W, Pastor-Pérez L, Shen DK, et al. Catalytic Upgrading of Biomass Model Compounds: Novel Approaches and Lessons Learnt from Traditional Hydrodeoxygenation – a Review. ChemCatChem 2019;11:924–60. https://doi.org/10.1002/cctc.201801722.

[16] Wang X, Zhang Z, Yan Z, et al. Catalysts with metal-acid dual sites for selective hydrodeoxygenation of lignin derivatives: Progress in regulation strategies and applications. Appl Catal A Gen 2023;662. https://doi.org/10.1016/j.apcata.2023.119266.

[17] Gollakota ARK, Shu CM, Sarangi PK, et al. Catalytic hydrodeoxygenation of bio-oil and model compounds - Choice of catalysts, and mechanisms. Renewable and Sustainable Energy Reviews 2023;187. https://doi.org/10.1016/j.rser.2023.113700.

[18] Vandevyvere T, Sabbe MK, Mendes PSF, et al. NiCu-based catalysts for the low-temperature hydrodeoxygenation of anisole: Effect of the metal ratio on SiO2 and γ-Al2O3 supports. Green Carbon 2023;1:170–84. https://doi.org/10.1016/j.greenca.2023.10.001.

[19] Poissonnier J, Ranga C, Lødeng R, et al. Oxygen functionality and chain length effects in HDO: Impact of competitive adsorption on reactivity. Fuel 2022;308:121940. https://doi.org/10.1016/j.fuel.2021.121940.

[20] Gracia J, Ayala-Cortés A, Di Stasi C, et al. Highly selective catalytic hydrodeoxygenation of guaiacol to benzene in continuous operation mode. Fuel Processing Technology 2024;255:108064. https://doi.org/10.1016/j.fuproc.2024.108064.

[21] Moura LG, dos Santos GES, Alves HO, et al. Hydrogenation of Guaiacol and Pyrolysis of Biomass Using Nickel and Niobium-Based Catalysts. Catal Letters 2024;154:2976–88. https://doi.org/10.1007/s10562-023-04500-1.

[22] Han Y, Pires APP, Garcia-Perez M. Co-hydrotreatment of the Bio-oil Lignin-Rich Fraction and Vegetable Oil. Energy & Fuels 2020;34:516–29. https://doi.org/10.1021/acs.energyfuels.9b03344.

[23] Denson MD, Manrique R, Olarte M, et al. Co-hydrotreatment of Bio-oil and Waste Cooking Oil to Produce Transportation Fuels. Energy & Fuels 2024;38:6982–91. https://doi.org/10.1021/acs.energyfuels.3c05176.

[24] Kikhtyanin O, Smirnov A, Korolova V, et al. Inhibiting effects during the co-conversion of lauric acid and anisole over Ni and NiMo catalysts. Appl Catal A Gen 2024;685:119889. https://doi.org/10.1016/j.apcata.2024.119889.

[25] Hočevar B, Grilc M, Huš M, et al. Mechanism, ab initio calculations and microkinetics of straight-chain alcohol, ether, ester, aldehyde and carboxylic acid hydrodeoxygenation over Ni-Mo catalyst. Chemical Engineering Journal 2019;359:1339–51. https://doi.org/10.1016/j.cej.2018.11.045.

[26] Hočevar B, Grilc M, Huš M, et al. Mechanism, ab initio calculations and microkinetics of hydrogenation, hydrodeoxygenation, double bond migration and cis–trans isomerisation during hydrotreatment of C6 secondary alcohol species and ketones. Appl Catal B 2017;218:147–62. https://doi.org/10.1016/j.apcatb.2017.06.046.

[27] Li M, Xing S, Yang L, et al. Nickel-loaded ZSM-5 catalysed hydrogenation of oleic acid: The game between acid sites and metal centres. Appl Catal A Gen 2019;587:117112. https://doi.org/10.1016/j.apcata.2019.117112.

[28] Liu Z, Mei J, Kong X, et al. Revealing the mechanism of selective hydrogenation of oleic acid on bifunctional hierarchical catalysts. J Catal 2025;450:116274. https://doi.org/10.1016/j.jcat.2025.116274.

[29] Kikhtyanin O, Kubička D. Understanding the different deoxygenation reaction pathways of lauric acid over alumina-supported Ni and Co catalysts. Sustain Energy Fuels 2023;7:485–501. https://doi.org/10.1039/D2SE01477G.

[30] Song W, Liu Y, Baráth E, et al. Dehydration of 1-Octadecanol over H-BEA: A Combined Experimental and Computational Study. ACS Catal 2016;6:878–89. https://doi.org/10.1021/acscatal.5b01217.

[31] Sedtabute S, Vitidsant T, Ngamcharussrivichai C. Production of jet fuel-range bio-hydrocarbons over nickel-based catalysts through hydrothermolysis without external H2: Effect of nanoporous supports. Energy Convers Manag

2025;331:119679. https://doi.org/10.1016/j.enconman.2025.119679.

[32] Korica N, Mendes PSF, De Clercq J, et al. Interplay of Metal-Acid Balance and Methylcyclohexane Admixture Effect on *n*-Octane Hydroconversion over Pt/HUSY. Ind Eng Chem Res 2021;60:12505–20. https://doi.org/10.1021/acs.iecr.1c01775.

[33] Pfrang C, Shiraiwa M, Pöschl U. Coupling aerosol surface and bulk chemistry with a kinetic double layer model (K2-SUB): oxidation of oleic acid by ozone. Atmos Chem Phys 2010;10:4537–57. https://doi.org/10.5194/acp-10-4537-2010.

[34] Wang R, Xia C, Peng B. Fundamental understanding and catalytic applications of hollow MFI-type zeolites. Catal Today 2022;405–406:111–24. https://doi.org/10.1016/j.cattod.2022.06.026.

[35] He P, Li L, Shao Y, et al. Recent Advances in Hydrodeoxygenation of Lignin-Derived Phenolics over Metal-Zeolite Bifunctional Catalysts. ChemCatChem 2024;16. https://doi.org/10.1002/cctc.202301681.

[36] Abreu Teles C, Duong N, Rabelo-Neto RC, et al. Evidence of dependence between the deoxygenation activity and metal–support interface. Catal Sci Technol 2022;12:5961–9. https://doi.org/10.1039/D2CY00969B.

View Article Online DOI: 10.1039/D6CY00118A

[37] Furimsky E, E Massoth F. Deactivation of hydroprocessing catalysts. Catal Today 1999;52:381–495. https://doi.org/10.1016/S0920-5861(99)00096-6.

[38] Yan P, Drewery M, Mensah J, et al. Study on Catalyst Deactivation During the Hydrodeoxygenation of Model Compounds. Top Catal 2020;63:778–92. https://doi.org/10.1007/s11244-020-01310-2.

[39] Abreu Teles C, Ciotonea C, Le Valant A, et al. Optimization of catalyst activity and stability in the m-cresol hydrodeoxygenation through Ni particle size control. Appl Catal B 2023;338:123030. https://doi.org/10.1016/j.apcatb.2023.123030.

[40] Ogliaruso M, Wolfe J. The synthesis of carboxylic acids and esters and their derivatives, 1991, p. 145–8. https://doi.org/10.1002/9780470772423.ch1.

[41] Venditto NJ, Liang YS, El Mokadem RK, et al. Ketone–Olefin Coupling of Aliphatic and Aromatic Carbonyls Catalyzed by Excited-State Acridine Radicals. J Am Chem Soc 2022;144:11888–96. https://doi.org/10.1021/jacs.2c04822.

View Article Online
DOI: 10.1039/D6CY00118A

Data availability

The raw and processed data for Fig. 2 – 3 are openly available in a FAIR format in *Zenodo* at https://doi.org/10.5281/zenodo.18313041. Details of data postprocessing are provided in Section 1 of ESI. Additional processed data supporting this study are included in ESI.